RoF-Based Mobile Fronthaul Networks Implemented by Using DML and EML for 5G Wireless Communication Systems

Byung Gon Kim 🆔, Sung Hyun Bae, Hoon Kim 🆔, *Senior Member, IEEE*, and Yun C. Chung 🆔, *Fellow, IEEE*

Abstract—We investigate the feasibility of implementing a mobile fronthaul network (MFN) based on the radio-over-fiber (RoF) technology for the fifth generation wireless communication systems cost effectively by using either directly modulated lasers (DMLs) or electroabsorption modulated lasers (EMLs) operating in the 1.55-μm window. The results show that the performance of the RoF-based MFN implemented by using DMLs is primarily limited by the composite second-order (CSO) distortions arising from the interplay between the DML's adiabatic chirp and fiber's chromatic dispersion. Thus, when we implement the RoF-based MFN by using the currently available commercial DML, its reach could be limited to ∼5 km due to the CSO distortions. To increase this reach, we can utilize the DML having a very small adiabatic chirp (or the optical dispersion compensation or CSO cancelation technique). On the other hand, when we implement the RoF-based MFN by using EML, its performance is limited mostly by the relatively poor linearity and low output power of EML rather than the chirp. For example, if we increase the optical modulation index to compensate for the low output power of EML, the distortions caused by the EML's nonlinear transfer curve can also be increased. Thus, for the use in the RoF-based MFN, it would be highly desirable to increase the output power of EML as much as possible. For a demonstration, we successfully transmit 24 100-MHz-bandwidth filtered orthogonal-frequency-division-multiplexing signals over 20 km of the standard single-mode fiber by using an EML transmitter with 7-dBm output power.

Index Terms—Directly modulated laser (DML), electro-absorption modulated laser (EML), filtered OFDM, mobile fronthaul network, radio-over-fiber (RoF).

I. INTRODUCTION

THE radio-over-fiber (RoF) technology has recently attracted significant attention as an alternative transport technology for the mobile fronthaul network (MFN) of the 5th generation (5G) wireless communication systems [1]–[15]. This is mainly due to the extremely large capacity required in such a network. For example, for the use in the 5G systems, the transmission capacity of the conventional MFN implemented by using the digital fiber-optic interfaces such as the Common Public Radio Interface (CPRI) would exceed hundreds of Gbps [8]–[15]. In comparison, by using the RoF technology, it would be possible to implement the MFN by using the optical transceivers having only about a few GHz of bandwidth.

Previously, it has been reported that the RoF-based MFN for the 4G wireless systems could be implemented cost-effectively by using a directly modulated laser (DML) [1]–[7]. However, in the case of using a DML for the implementation of the RoF-based MFN to be used in the 5G systems, its performance can be seriously limited by the composite second-order (CSO) distortions caused by the interplay between the DML's chirp and the chromatic dispersion of optical fiber due to the much larger bandwidth requirement of the 5G signals compared to the 4G signals [8], [9]. Thus, up till now, the RoF-based MFN for the 5G systems has been demonstrated mostly by using a Mach-Zehnder modulator (MZM) [10]–[15]. This is because the MZM can generate a chirp-free signal, which is critical for mitigating the effects of the fiber's chromatic dispersion, and has a relatively good linearity. However, considering its high cost and the fact that there will be numerous cell sites to be connected by MFN (since the cell densification will be increasingly important in the 5G systems), it would be highly desirable if we could utilize cost-effective optical transmitters such as DMLs or electro-absorption modulated lasers (EMLs) instead of using the expensive MZM-based optical transmitters.

In this paper, we investigate the feasibility of implementing the RoF-based MFN for the 5G systems by using either DML or EML. For this purpose, we assume that the MFN should transport twenty-four 100-MHz-bandwidth filtered-orthogonal-frequency-division-multiplexing (f-OFDM) signals (which are one of the waveform candidates for the 5G systems) [16]–[18]. We then evaluate the performance of these signals after the transmission over the standard single-mode fiber (SSMF). From these results, we identify the requirements of DML and EML for the use in the RoF-based MFN. However, it should be noted that, in this paper, we report on the performance of the DML and EML operating in the 1.55-μm window only. This is because, to enhance the cost-effectiveness of MFN, it is critical to utilize the full-duplex bidirectional transmission technique by using both 1.3- and 1.55-μm windows. However, we can realize the
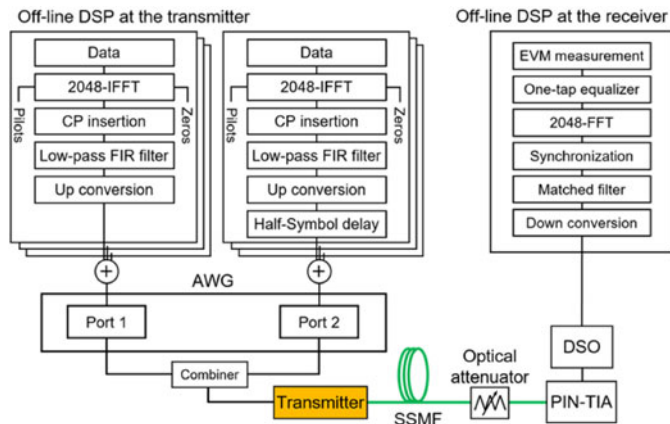
Fig. 1. Experimental setup.

Fig. 2. RF spectra of OFDM and f-OFDM signals.

1.3-μm RoF link by using DML or EML without much technical difficulties, despite their chirps, due to the low dispersion of SSMF at this window. Thus, we focus our investigation on the feasibility of implementing the RoF-based MFN by using the DML or EML operating in the 1.55-μm window.

II. EXPERIMENTAL SETUP

Although the 5G wireless communication system is expected to be deployed at about the year 2020, its standardization is yet to be completed [19], [20]. However, at the least, it is clear now that the peak cell capacity of the 5G systems should be larger than 10 Gbps [16]. Thus, in this study, we assumed that the 5G system should be able to provide a peak cell capacity of 14.4 Gbps by using 3 sectors, 8 × 8 multiple-input multiple-output (MIMO) antennas, and 100-MHz-bandwidth channel f-OFDM signals in 64 quadrature amplitude modulation (64-QAM) format. In this case, the RoF-based MFN should be capable of delivering the signals within 2.4 GHz (= 3 × 8 × 100 MHz). We evaluated the performances of these f-OFDM signals by using the error-vector magnitude (EVM), assuming that it should be better than 8% (since this value corresponds to the uncorrected bit-error rate of 10^{-3} for 64-QAM signal). We also note that this value is identical to the EVM requirement for 64-QAM signal stipulated in the 3rd generation partnership project (3GPP) specifications [20].

Fig. 1 shows the experimental setup. We first generated an OFDM symbol by taking 2048 inverse fast Fourier transform (IFFT) of 1000 data subcarriers modulated in 64-QAM format and 200 pilot subcarriers in the quadrature phase-shift keying (QPSK) format. The subcarrier spacing was set to be 83.3 kHz. Thus, the signal occupied a bandwidth of 100 MHz (= 83.3 kHz × 1200). We then added a 7% cyclic prefix (CP) to this 12-μs OFDM symbol. For the generation of the f-OFDM signal (by filtering out the spectral leakage of the OFDM signal), we utilized an ideal low-pass filter truncated by the 1024-tap Hamming window. The bandwidth of this low-pass finite impulse response (FIR) filter was set to be 100.5 MHz. Fig. 2 shows the RF spectra of the generated OFDM and f-OFDM signals. In the case of the conventional OFDM signal, a large spectral leakage was observed outside of the signal band due to its rectangular windowing. By contrast,
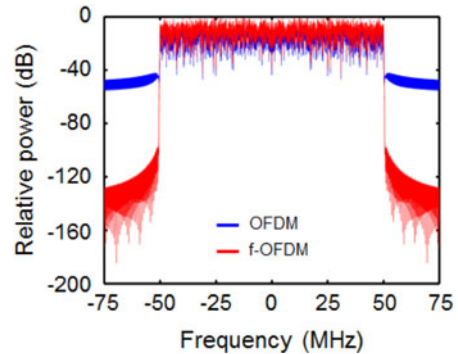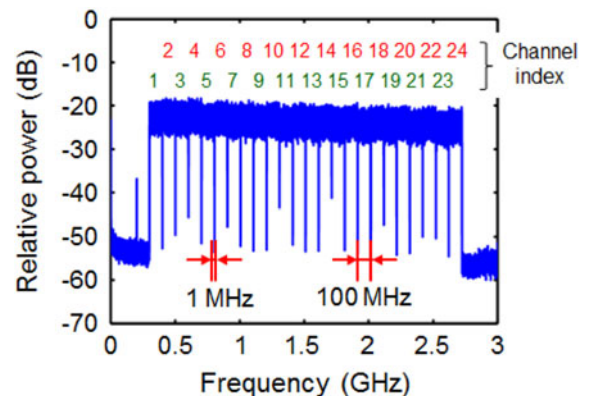

Fig. 3. RF spectrum of the 24 f-OFDM signals measured at the output of the RF power combiner.

in the case of the f- OFDM signal, this spectral leakage was measured to be >80 dB lower than the conventional OFDM signal. This spectrally localized f-OFDM signal enabled us to minimize the guard band between the signals, and, as a result, to enhance the spectral efficiency. We generated twenty-four of this 100-MHz-bandwidth f-OFDM signal off-line and ported them to an arbitrary waveform generator (AWG). The carrier frequencies of these twenty-four f-OFDM signals were positioned at $350 + 101 \times (i - 1)$ MHz, where i is the channel index ranging from 1 to 24. The signals with odd channel indices were generated from port 1 of the AWG, while the signals with even channel indices were generated from port 2. To simulate the asynchronous transmission between adjacent channels, we inserted a 6.4-μs time delay in port 2. The signals generated from the AWG were then combined by using an RF power combiner. Fig. 3 shows the RF spectrum of the 24 f-OFDM channels measured at the output of the RF combiner. The guard band was set to be only 1 MHz, which was 1% of the channel bandwidth. It is interesting to note that the guard band of the 4th generation LTE-A signal accounts for 10% of the channel bandwidth [17], [20]. The 24 f-OFDM signals were applied to a cost-effective optical transmitter (i.e., DML or EML), operating at ∼1550 nm. After the transmission over up to 20 km of SSMF, the signals were detected by using a PIN receiver. We set the optical power incident on the receiver to be −2 dBm regardless of the transmission distance, since the nonlinear distortions caused by the saturation of the receiver were observed at beyond this optical power. The received signals were digitized by using a digital

sampling oscilloscope (DSO) at 40 Gsample/s. In the off-line signal processing, we first down-converted the detected signals into the baseband and passed them through the matched filter. We then demodulated the signals by taking FFT and measured the EVM performance after one-tap equalization.

III. RESULTS

A. Directly Modulated Laser (DML)

It has been recently reported that, when we implement the RoF-based MFN for the 5G system by using a 1.55-μm DML, its performance is limited primarily by the dispersion-induced CSO distortions [8], [9]. The CSO distortions depend strongly on the chirp characteristics of DML. However, to the best of our knowledge, the effect of the DML's chirp on the RoF-based MFN has not been reported yet. Thus, we attempt to estimate the chirp parameters of DML required for the implementation of the RoF-based MFN (by suppressing the CSO distortions).

The carrier-to-distortion ratio (CDR) of a subcarrier channel limited by the CSO distortions in the RoF-based MFN can be described as [5]

$$CDR \simeq \frac{\eta^2 + (\omega_i \pm \omega_k)^2 (P_{\mathrm{avg}}\theta\beta_{FM})^2}{N_{\mathrm{CSO}}m^2 P_{\mathrm{avg}}{}^2 \times (\omega_i \pm \omega_k)^2 (\theta\beta_{FM})^2} \quad (1)$$

where ω_i is the angular frequency of the ith channel, N_{cso} is the two-tone product count, P_{avg} is the average output power, m is the optical modulation index (OMI) per channel, and η and β_{FM} represent the slope efficiency and frequency modulation (FM) efficiency of DML, respectively. Also, θ is given by $DL\lambda^2/c$, where D is the dispersion parameter, L is the transmission distance, λ is the wavelength, and c is the velocity of light. By using this equation, we estimated the chirp parameters of a DML required for the implementation of the RoF-based MFN. For this purpose, we first expressed the FM efficiency, β_{FM}, in terms of the DML's chirp parameters as follows.

The instantaneous frequency shift of DML can be expressed as [21]

$$\Delta\nu = -\frac{\alpha}{4\pi}\left(\frac{d}{dt}\ln P(t) + \kappa P(t)\right) \quad (2)$$

where $P(t)$ is the instantaneous optical power of DML, α is the linewidth enhancement factor, and κ is the adiabatic chirp coefficient. Thus, by using the small-signal approximation and time-harmonic analysis, we can express the FM efficiency of DML as

$$\beta_{FM}(\omega) = \frac{\Delta\nu}{\Delta i} = -\frac{\alpha\eta}{4\pi}\left(\frac{1}{P_{\mathrm{avg}}}j\omega + \kappa\right). \quad (3)$$

Then, the FM efficiency can be approximated as

$$\beta_{FM} \simeq -\frac{\alpha\eta\kappa}{4\pi} \quad (4)$$

if $\omega/P_{\mathrm{avg}} \ll \kappa$. In our case, there is no problem in satisfying this condition, considering the highest frequency of the signal used in this work (2.7 GHz) and the typical adiabatic chirp parameter, κ, of a commercial DML (i.e., $\kappa = 3.2 \sim 15$ GHz/ mW) [22]–[24]. Thus, by using (1) and (4), the CDR limited by the CSO distortions can be estimated as functions of the DML's chirp parameters, α and κ. On the other hand, the EVM performance

of the RoF link can be estimated from the carrier-to-noise-and-distortion ratio (CNDR) since

$$EVM = 1/\sqrt{CNDR}. \quad (5)$$

This is because the nonlinear distortions can be regarded as the equivalent Gaussian noises in wideband multi-carrier systems [24], [25]. In this equation, we considered the carrier-to-noise ratio (CNR) limited by the receiver's thermal and shot noises as well as the CDR determined by (2). However, as expected, CDR became dominant over CNR as the transmission distance increased (due to the increased CSO distortions). Fig. 4 shows the contour plots of the EVM performances estimated as functions of α and κ at various transmission distances. In this figure, we showed only the EVM performances of channel 24 since the highest-frequency channel would suffer the most from the CSO distortions. For this estimation, we used the same parameters as in our experiment (i.e., $\lambda = 1551$ nm, $\eta = 0.17$ W/A, $D = 17$ ps/nm/km, $P_{\mathrm{avg}} = 9.2$ dBm, and $m = 4.3\%$). The shaded areas in this figure indicate the range of the typical chirp parameters of commercial DMLs (i.e., $\alpha = 2.4 \sim 5.2$ and $\kappa = 3.2 \sim 15$ GHz/mW) [22]–[24]. The chirp parameters of the DML used in our experiment are also shown in this figure.

To satisfy the 8% EVM requirement for 64-QAM signal, the RoF-based MFN should be able to provide the CNDR of >22 dB. By using this CNDR requirement, we could identify the DML's chirp parameters required for the implementation of the RoF-based MFN. For example, when the fiber length is 5 km, the product of α and κ should be smaller than ~47 GHz/mW to achieve the CNDR of 22 dB. The results in Fig. 4(a) show that most commercial DMLs can satisfy this condition except those having both very large α and κ. However, when the fiber length is increased to 10 km, it appears that the DMLs should be carefully selected for the use in the RoF-based MFN as the requirement of the product of α and κ is substantially reduced to ~21 GHz/mW, as shown in Fig. 4(b). When the fiber length is increased further to 20 km, this problem becomes much more serious as the product of α and κ should be smaller than ~11 GHz/mW. As shown in Fig. 4(c), almost no commercial laser can satisfy this condition. Thus, for the implementation of the 20-km long RoF-based MFN by using a 1.55-μm DML, it would be inevitable to use the optical dispersion compensation [8], the intermediate frequency (IF) optimization [3], [8], or the CSO cancellation technique [9]. In Fig. 4, we also noted that it would be desirable to utilize the DML having small α and κ to suppress the CSO distortions. However, the adiabatic chirp parameter, κ, could be changed by tailoring the laser structure [21], [27]. Thus, if necessary, we should be able to fabricate the DML to have a small κ for the use in the RoF-based MFN.

To verify the results in Fig. 4, we measured the performance of the RoF-based MFN implemented by using a 1.55-μm DML and the experimental setup shown in Fig. 1. In this experiment, we intentionally utilized a 1.55-μm DML with an exceptionally small adiabatic chirp parameter, κ, of only 3.2 GHz/mW. The linewidth enhancement factor, α, of this laser was measured to be 3.6. When we set the bias current of this DML to be 65 mA, its output power, wavelength, and slope efficiency were measured to be 9.2 dBm, 1551 nm, and 0.17 W/A, respectively. Fig. 5
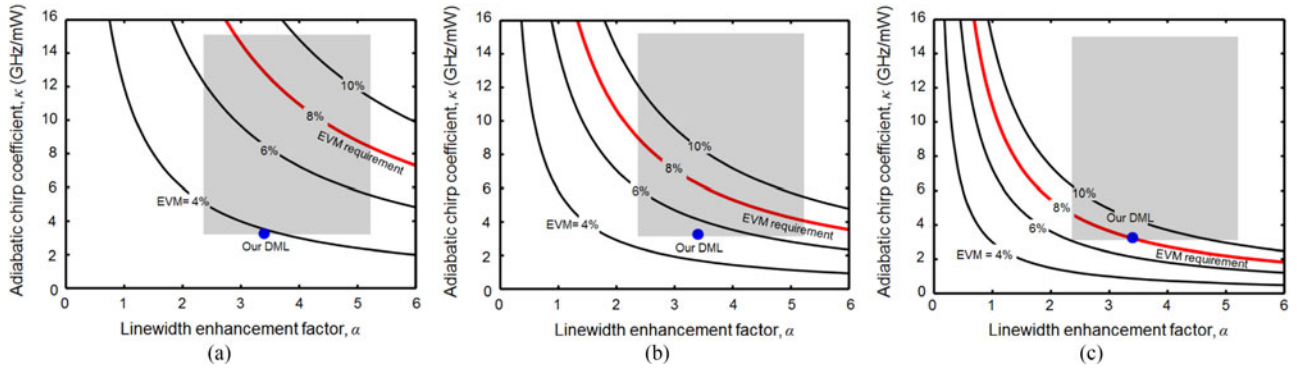
Fig. 4. EVM performance of channel 24 in the RoF-based MFN implemented by using 1.55-μm DML estimated as functions of α and κ when the transmission fibers are (a) 5 km, (b) 10 km, and (c) 20 km long. In this estimation, the output power of the DML and root-mean-square OMI were assumed to be 9 dBm and 20%, respectively.
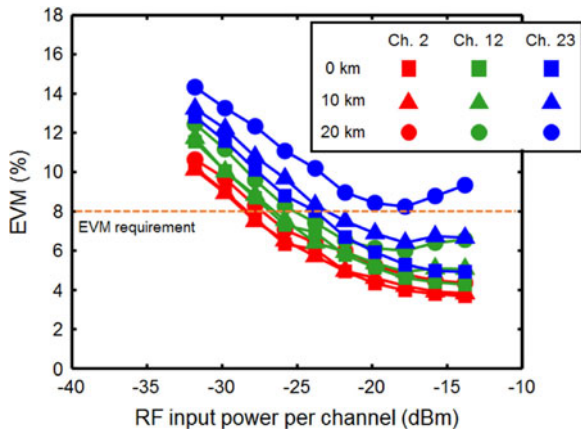

Fig. 5. EVM performances of 3 exemplary channels measured as a function of RF power per channel in the RoF-based MFN implemented by using a 1.55-μm DML.

shows the measured EVM performances of 3 channels (operating at low, middle, and high frequencies) as a function of the RF power per channel for various transmission distances. When the RF input power per channel was larger than -13.8 dBm, we could not measure the EVM performances due to the limited saturation power of the laser driver. The results show that, as expected, the EVM performance was improved with the RF power of the signal in the case of back-to-back transmission. However, as we increased the transmission distance, the performance of the high-frequency channel was deteriorated due to the dispersion- induced CSO distortions. For example, after the transmission over 20 km of SSMF, the EVM performance of channel 23 was degraded to be worse than 8% and, as a result, could not satisfy the EVM requirement. From these results, we confirmed that the EVM performances of the high-frequency channels could be seriously affected by the CSO distortions even when we utilized the DML having an exceptionally small adiabatic chirp coefficient, κ, of 3.2 GHz/mW.

Fig. 6 shows the RF spectra of 24 f-OFDM signals measured at the receiver. The second-order intermodulation distortions could be easily observed at outside of the signal's band as they were spread up to twice the highest signal frequency (i.e., 2×2.673 GHz $= 5.346$ GHz). No significant CSO distortion was observed in the back-to-back condition, while it was in-
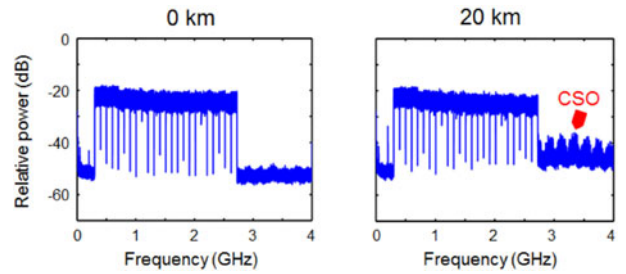

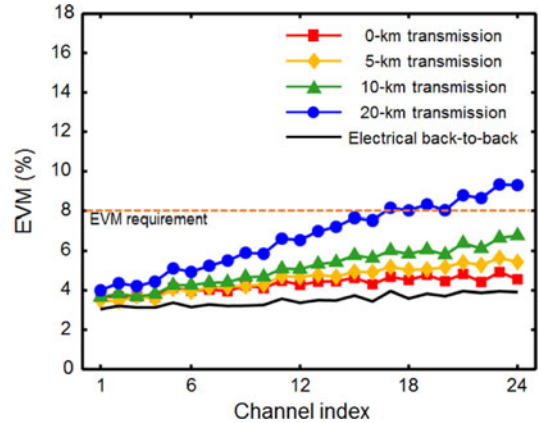Fig. 6. RF spectra of 24 f-OFDM signals measured at the receiver in the RoF link implemented by using 1.55-μm DML.

Fig. 7. EVM performances of all 24 channels measured at various transmission distances in the RoF link implemented by using 1.55-μm DML. The RF power per channel was set to be -13.8 dBm.

creased to be about 10 dB higher than the noise floor after the 20-km long SSMF transmission. This figure also showed that the dispersion-induced RF power fading was not as severe as the CSO distortions since the received RF power of the highest-frequency channel (i.e., channel 24 at 2.67 GHz) was reduced by <1 dB even after the transmission over 20 km of SSMF. Fig. 7 shows the EVM performance of all 24 channels measured after setting the RF power per channel to be -13.8 dBm. In the back-to-back condition, the EVM performance was measured to be almost uniform across the entire channel. However, as the transmission distance was increased, a gradual degradation was observed in the EVM performances of high-frequency channels

due to the dispersion-induced CSO distortions. As a result, after the transmission over 20 km of SSMF, the high-frequency channels at >2 GHz (i.e., channel index: >18) could not satisfy the 8% EVM criterion. For example, after the transmission over 20 km of SSMF, the EVM performance of channel 24 was measured to be 9.3%. In any case, the results in Figs. 4 and 7 indicated that, as long as the maximum transmission distance is shorter than 10 km, we could realize the RoF-based MFN by utilizing the 1.55-μm DML having small chirp parameters (i.e., the product of α and κ should be smaller than $\sim$21 GHz/mW). However, when the transmission distance should be increased to be longer than 20 km, it is crucial to utilize the optical dispersion compensation or the CSO cancellation technique for the implementation of the RoF-based MFN by using a 1.55-μm DML.

Fig. 7 also shows the electrical EVM performances measured in back-to-back condition by directly connecting the output of AWG to the input of DSO. Thus, these EVM performances were limited mostly by the quantization noises of the AWG and DSO used in this experiment. Since the measured EVM values were in the range of 3.3 ~ 4.0%, we could not use the higher-level formats than 64-QAM (such as 256-QAM, which required the 3.5% EVM threshold). However, if necessary, we should be able to improve the EVM performance to support 256-QAM format by reducing the quantization noises (i.e., by increasing the resolution of the analog-to-digital converters and digital-to-analog converters) or reducing the peak-to-average power ratio (PAPR) of the OFDM signals.

B. Electro-Absorption Modulated Laser (EML)

As described above, the performance of the RoF-based MFN implemented by using a 1.55-μm DML could be limited by the CSO distortions arising from the interplay between the laser's adiabatic chirp and fiber's chromatic dispersion. Thus, one potential solution to avoid this problem would be the use of a 1.55-μm EML, instead of a DML, since it has no adiabatic chirp. This solution could also help to mitigate the deleterious effects of the dispersion-induced RF power fading since an EML has a small linewidth enhancement factor [28]. As a result, in this case, the system's performance could be limited mostly by the nonlinearity in the EML's transfer curve. Previously, various techniques have been proposed to mitigate the distortion caused by this nonlinearity, including the dual-wavelength technique [29], mixed polarization technique [30], optical feed-forward technique [31], and electronic pre-distortion [32]. However, the use of these techniques could increase the system's cost and complexity. Thus, in this paper, we evaluated the feasibility of implementing an RoF-based MFN by using an EML without using these linearization techniques.

We estimated the nonlinearity of EML's transfer curve by using Taylor series [33]. Thus, the OMI and the CDR limited by the nonlinear transfer curve of EML can be expressed as [33]

$$\text{OMI} = (h_1/h_0) \times V \tag{6}$$

$$\text{CDR} = \left[(h_1 V)^2 / \left\{ N_{\text{CSO}} (h_2 V^2)^2 \right\} \right] \tag{7}$$
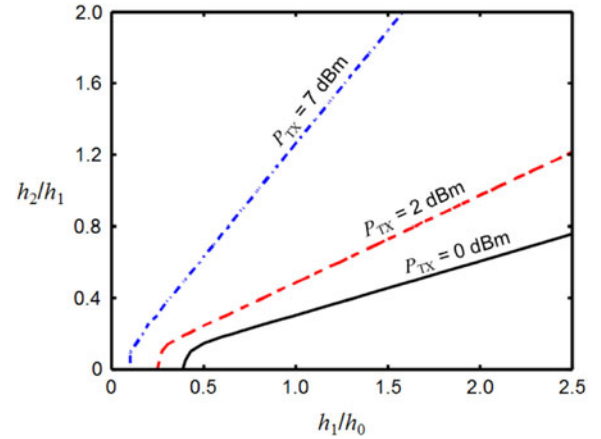

Fig. 8. A contour plot of the 8% EVM performances estimated as functions of OMI (h_1/h_0) and nonlinearity (h_2/h_1) of EML for various output powers of the EML transmitter. In this estimation, the link loss was assumed to be 9 dB.

where h_i is the ith-order coefficient in the EML's transfer curve expanded by Taylor series and V is the voltage applied to the electro-absorption modulator (EAM) section of the EML. In these equations, we noted that the (h_1/h_0) and (h_2/h_1) terms could determine the OMI and the nonlinearity of EML, respectively. In other words, the OMI and the nonlinearity of EML increased with these terms. By using (5), (6), and (7), we estimated the EVM performance of the EML-based RoF link as functions of (h_1/h_0) and (h_2/h_1). In this estimation, we assumed that the link loss was 9 dB (i.e., 5 dB for 20-km long SSMF, 2 dB for two 1.3/1.55-μm couplers, and 2 dB for the system margin). Fig. 8 shows a contour plot of the 8% EVM performances estimated as functions of the OMI (i.e., h_1/h_0) and nonlinearity of EML (i.e., h_2/h_1) for various output powers of the EML transmitter (P_{TX}). From this figure, we found that the usable ranges of the EML's parameters (such as OMI and linearity) to satisfy the 8% EVM requirement for 64-QAM signal increased significantly with P_{TX}. This result also indicated that, if P_{TX} was high enough, we could implement the RoF-based MFN by using practically any EMLs (i.e., regardless of their OMIs and nonlinearities). For example, if we could increase P_{TX} to 7 dBm, there should be no problem in satisfying the 8% EVM requirement even when the RoF-based MFN was implemented by using an extremely nonlinear EML (i.e., $h_2/h_1 \approx 1$ V [30]).

To verify our estimation, we implemented an RoF link by using a 1.55-μm EML. Fig. 9 shows the transfer curve of the EML used in this experiment. For this measurement, we biased the laser section of this EML at 70 mA and set the bias voltage of the EAM section at -1 V. Under these conditions, the output power of this EML was measured to be 2 dBm. The transfer curve of this EML can be expressed by using an exponential function as [30]

$$P_{\text{EML}} = \exp\left(1.468 + 0.455\,V - 0.4128\,V^2 + 0.150\,V^3\right) \tag{8}$$

The fitted curve by using this equation agreed very well with the measured data, as shown in Fig. 9. At around the bias voltage of -1 V, this transfer curve can be approximated by using Taylor
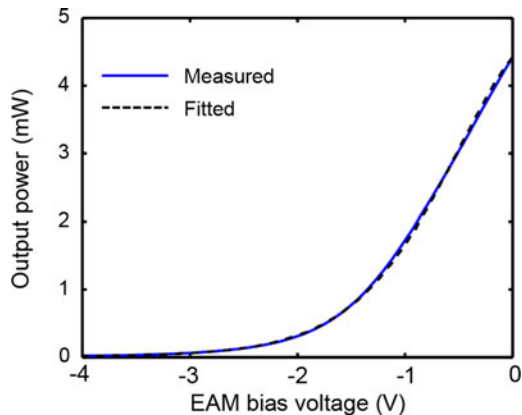
Fig. 9. Measured transfer curve of the 1.55-μm EML used in this experiment in comparison with a fitted curve. The laser section of this EML was biased at 70 mA.

series as

$$P_{\text{EML}} \simeq 1.66 + 2.35\,(V+1) + 1.11(V+1)^2 \qquad (9)$$

Thus, the (h_1/h_0) and (h_2/h_1) terms of this EML were determined to be 1.42 and 0.472 V, respectively. Accordingly, we surmised from Fig. 8 that, to satisfy the 8% EVM criterion in the 20-km long RoF-based MFN, the output power of this EML should be higher than $\sim$2 dBm.

We evaluated the effects of the output power of the EML transmitter (P_{TX}) on the EVM performances of the RoF-based MFN. For this purpose, we measured the EVM performances of twenty-four 100-MHz-bandwidth f-OFDM signals in the 20-km long RoF link after setting the output power of the EML transmitter to be either 2 or 7 dBm. However, in this measurement, we did not increase this output power to be higher than 7 dBm to avoid the performance degradations caused by the stimulated Brillouin scattering (SBS) [34]. Fig. 10 shows the measured EVM performances of three exemplary channels in comparison with the theoretically calculated curves by using (5), (6), and (7). As expected, when we set the output power of the EML transmitter to be 2 dBm, it was difficult to satisfy the 8% EVM requirement (since it was necessary to set the RF input power per channel to be precisely at -24 dBm), as shown in Fig. 10(a). However, when we boosted up the output power to 7 dBm by using an erbium-doped fiber amplifier, we could easily satisfy the 8% EVM requirement by using a wide range of the RF input power per channel, as shown in Fig. 10(b). In these figures, the discrepancies between the measured data and calculated curve were observed at high-frequency channels due to the poor high-frequency response characteristics of the EML used in this experiment (i.e., the frequency response of this EML at 2.7 GHz was measured to be 1.5 dB lower than the value at DC).

Fig. 11 shows the optimal EVM performances of 24 channels measured after the SSMF transmission. For this measurement, we set the RF power per channel to be -26 dBm and the optical power launched into the SSMF to be 7 dBm. The result showed that the EVM performances were nearly unchanged even after the transmission over 20 km of SSMF. This was because the transmission performance of the EML-based RoF link was not
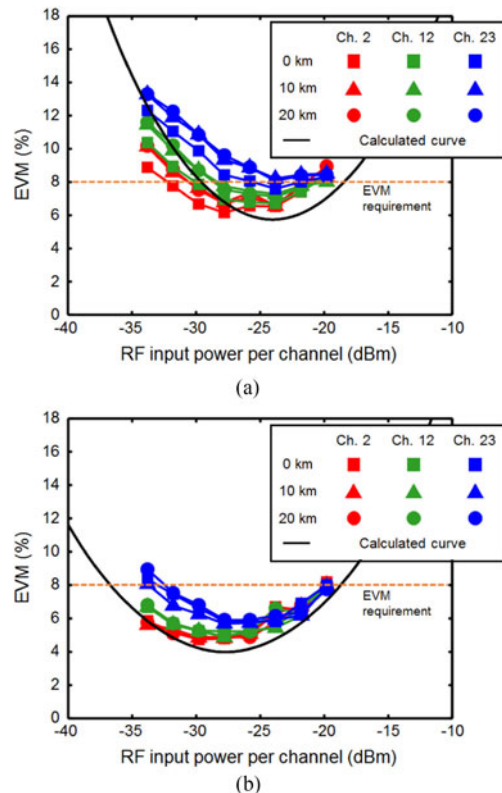

Fig. 10. EVM performances as a function of the RF power per channel in the 20-km long RoF link implemented by using 1.55-μm EML. (a) $P_{TX} = 2$ dBm and (b) $P_{TX} = 7$ dBm.
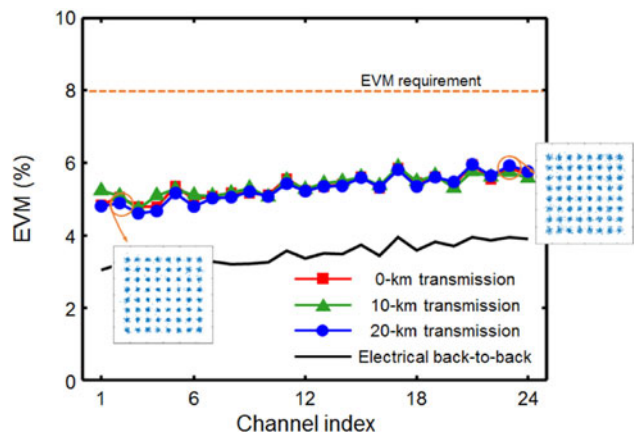

Fig. 11. EVM performances of 24 100-MHz-bandwidth f-OFDM signals measured in the RoF link implemented by using 1.55-μm EML.

affected by the dispersion-induced CSO distortions (since EML had no adiabatic chirp). As a result, all the 24 channels could satisfy the 8% EVM requirement for 64-QAM signal regardless of the transmission distances.

IV. SUMMARY

We have evaluated the possibility of implementing the RoF-based MFN for the 5G systems cost-effectively by using either DML or EML operating in the 1.55-μm window. In particular, we attempted to evaluate the achievable performances in such networks without using any complicated mitigation methods

(e.g., for the dispersion-induced CSO distortion in the case of using DML and the nonlinear transfer curve in the case of using EML). In this evaluation, we assumed that the MFN should be capable of transporting twenty-four 100-MHz-bandwidth f-OFDM signals modulated in 64-QAM format for the use in the 5G systems.

When we implemented the RoF-based MFN by using DML, a superb transmission performance was observed in the back-to-back condition due to its excellent linearity. In addition, due to the DML's chirp, we could utilize the high optical power without inducing SBS. However, when we transmitted the f-OFDM signals through SSMF in this network, the system's performance was limited by the CSO distortions arising from the interplay between the DML's adiabatic chirp and fiber's chromatic dispersion. Thus, we developed a theoretical model to estimate the specifications of the DML's chirp parameters, α and κ, required for satisfying the 8% EVM criterion for 64-QAM signal. By using this model, we found that the products of α and κ should be less than 47 GHz/mW and 11 GHz/mW for the 5-km and 20-km reach RoF-based MFNs, respectively. This result indicated that we could implement the RoF-based MFN covering up to 5 km by using most of the currently available DMLs. However, when the transmission distance should be increased to ~10 km, it would be necessary to use the DMLs selected for (or fabricated to have) very small adiabatic chirp. If the transmission distance should be increased further to 20 km, it would be inevitable to utilize the optical dispersion compensation [8], the IF optimization [3], [8] or the CSO cancellation technique [9]. We experimentally confirmed these results by using a 1.55-μm DML having an exceptionally small adiabatic chirp coefficient of 3.2 GHz/mW.

In the case of implementing the RoF-based MFN by using EML, its performance would not be affected by the dispersion-induced CSO distortions (since EML has no adiabatic chirp). Instead, the performance of this network could be limited by the poor linearity and low output power inherent in the EML. We could increase the OMI to overcome the limitations caused by the low output power of EML. However, it would inevitably increase the distortions caused by the EML's nonlinear transfer curve, which, in turn, deteriorated the system's performance. Thus, for the use in the RoF-based MFN, it would be desirable to increase the output power of EML as much as possible (until the SBS-induced degradations developed). For example, our analytical results showed that, if we could increase the output power of EML to 7 dBm, it would be possible to implement the RoF-based MFN with 20-km reach by using even an extremely nonlinear EML (having $h_2/h_1 \approx 1$ V). In other words, we could implement the 20-km reach RoF-based MFN practically by using any EMLs regardless of their nonlinearities. Conversely, it would be possible to implement such MFN by using low-power EMLs if we could improve their linearity substantially. For the experimental verification of these results, we measured the EVM performances in a 20-km long RoF link implemented by using EML after setting its output power to be 2 and 7 dBm. The results showed that, when we set the output power of EML to be 2 dBm, it was difficult to satisfy the 8% EVM criterion. On the other hand, when we increased the output power to 7 dBm,

the 8% EVM requirement could be satisfied by using a wide range of amplitudes of the RF input signal applied to EML.

We summarized our findings as follows.

- As long as the transmission distance is shorter than 5 km, the RoF-based MFN can be implemented by using any commercial DMLs.
- When the transmission distance is shorter than 10 km, the RoF-based MFN can be implemented by using the DMLs fabricated to have a small adiabatic chirp.
- When the transmission distance is shorter than 20 km, the RoF-based MFN can be implemented by using the EMLs having sufficiently large output power.
- No mitigation technique is needed in these RoF-based MFNs.

In this paper, we assumed that the 5G systems would utilize twenty-four 100-MHz-bandwidth f-OFDM signals modulated in 64-QAM format. Thus, the aggregated signal bandwidth was <3 GHz. However, although this is plausible, the 5G systems could utilize higher signal bandwidth of >10 GHz and higher-level formats such as 256-QAM in the future. Even in such a case, the signal bandwidth would not be a problem since there are already many commercial of DMLs and EMLs having >10-GHz bandwidth. However, the achievable EVM could be limited by the PAPR. Thus, to support the large OFDM signals modulated in 256-QAM format, it would be necessary to utilize an effective PAPR reduction technique.

We believe that the results found in this work could help the cost-effective development of the RoF-based MFN for the 5G systems by using either DML or EML.

REFERENCES

[1] S. H. Cho, H. Park, H. S. Chung, K. H. Doo, S. Lee, and J. H. Lee, "Cost-effective next generation mobile fronthaul architecture with multi-IF carrier transmission scheme," in *Proc. Opt. Fiber Commun. Conf.*, San Francisco, CA, USA, Mar. 9–14, 2014, Paper Tu2B.6.

[2] X. Liu, H. Zeng, and F. Effenberger, "Experimental demonstration of high-throughput low-latency mobile fronthaul supporting 48 20-MHz LTE signals with 59-Gb/s CPRI-equivalent data rate and 2-μs processing delay," in *Proc. Eur. Conf. Opt. Commun.*, Valencia, Spain, Sep. 27–Oct. 1, 2015, Paper We.4.4.3.

[3] F. Effenberger and X. Liu, "Power-efficient method for IM-DD optical transmission of multiple OFDM signals," *Opt. Express*, vol. 23, no. 10, pp. 13571–13579, 2015.

[4] C. Han, S. H. Cho, H. S. Chung, and J. H. Lee, "Linearity improvement of direct-modulated multi-IF-over-fiber LTE-A mobile fronthaul link using shunt diode predistorter," in *Proc. Eur. Conf. Opt. Commun.*, Valencia, Spain, Sep. 27–Oct. 1, 2015, Paper We.4.4.4.

[5] X. Liu, F. Effenberger, N. Chand, L. Zhou, and H. Lin, "Demonstration of bandwidth-efficient mobile fronthaul enabling seamless aggregation of 36 E-UTRA-like wireless signals in a single 1.1-GHz wavelength channel," in *Proc. Opt. Fiber. Commun.*, Los Angeles, CA, USA, Mar. 22–26, 2015, Paper M2J.2.

[6] J. Zhang et al., "Memory-polynomial digital pre-distortion for linearity improvement of directly-modulated multi-IF-over-fiber LTE mobile fronthaul," in *Proc. Opt. Fiber. Commun.*, Anaheim, CA, USA, Mar. 20–24, 2016, Paper Tu2B.3.

[7] B. G. Kim, H. Kim, and Y. C. Chung, "Impact of multipath interference in the performance of RoF-based mobile fronthaul network implemented by using DML," *J. Lightw. Technol.*, vol. 35, no. 2, pp. 145–151, Jan. 2017.

[8] M. Sung, S. Cho, H. Chung, S. Kim, and J. Lee, "Investigation of transmission performance in multi-IFoF based mobile fronthaul with dispersion-induced intermixing noise mitigation," *Opt. Express*, vol. 25, no. 8, pp. 9346–9357, 2017.

[9] B. G. Kim, S. H. Bae, H. Kim, and Y. C. Chung, "DSP-based CSO cancellation technique for RoF transmission system implemented by using directly modulated laser," *Opt. Express*, vol. 25, no. 11, pp. 12152–12160, 2017.

[10] P. Dat, A. Kanno, N. Yamamoto, and T. Kawanishi, "190-Gb/s CPRI-equivalent rate fiber-wireless mobile fronthaul for simultaneous transmission of LTE-A and F-OFDM signals," in *Proc. Eur. Conf. Opt. Commun.*, Düsseldorf, Germany, Sep. 18–22, 2016, Paper W.4.P1.SC7.72.

[11] L. Cheng, X. Liu, N. Chard, F. Effenberger, and G. K. Chang, "Experimental demonstration of sub-Nyquist sampling for bandwidth- and hardware-efficient mobile fronthaul supporting 128×128 MIMO with 100-OFDM signals," in *Proc. Opt. Fiber Commun.*, Anaheim, CA, USA, Mar. 20–24, 2016, Paper W3C.3.

[12] J. Zhang et al., "Full-duplex quasi-gapless carrier aggregation using FBMC in centralized radio-over-fiber heterogeneous networks," *J. Lightw. Technol.*, vol. 35, no. 4, pp. 989–996, Feb. 2017.

[13] P. Dat, A. Kanno, N. Yamamoto, and T. Kawanishi, "Simultaneous transmission of multi-RATs and mobile fronthaul in the MMW bands over IFoF system," in *Proc. Opt. Fiber Commun.*, Los Angeles, CA, USA, Mar. 19–23, 2017, Paper W1C.4.

[14] M. Bi, W. Jia, L. Li, X. Miao, and W. Hu, "Investigation of F-OFDM in 5G fronthaul networks for seamless carrier-aggregation and asynchronous transmission," in *Proc. Opt. Fiber Commun. Conf.*, Los Angeles, CA, USA, Mar. 19–23, 2017, Paper W1C.6.

[15] S. Ishimura et al., "Simultaneous transmission aggregated microwave and millimeter-wave signals over fiber with parallel IM/PM transmitter for mobile fronthaul links," in *Proc. Eur. Conf. Opt. Commun.*, Gothenburg, Sweden, Sep. 17–21, 2017, Paper Tu.1.B.5.

[16] "IMT vision frame work and overall objectives of the future development of IMT for 2020 and beyond," ITU Radiocommunication, Geneva, Switzerland, ITU-R Recommendation M.2083-0, Sep. 2015.

[17] X. Zhang, M. Jia, L. Chen, J. Ma, and J. Qiu, "Filtered-OFDM—Enabler for flexible waveform in the 5th generation cellular networks," in *Proc. IEEE Global Commun. Conf.*, 2015, pp. 1–6.

[18] M. Abdoli, J. Ming Jia, and J. Ma, "Filtered OFDM: A new waveform for future wireless systems," in *Proc. Signal Process. Adv. Wireless Commun.*, 2015, pp. 66–70.

[19] "Study on new radio (NR) access technology," 3GPP, Sophia Antipolis Cedex, France, 3GPP TR 38.912 version 14.0.0, 2017.

[20] "Base station (BS) radio transmission and reception," 3GPP, Sophia Antipolis Cedex, France, 3GPP TS 36.104 version 14.3.0, 2017.

[21] T. Koch and R. Link, "Effect of nonlinear gain reduction on semiconductor laser wavelength chirping," *Appl. Phys. Lett.*, vol. 48, no. 10, pp. 613–615, 1986.

[22] S. H. Bae, H. Kim, and Y. C. Chung, "Transmission of 51.56 Gb/s OOK signal using 1.55-μm directly modulated laser and duobinary electrical equalizer," *Opt. Express*, vol. 24, no. 20, pp. 22555–22562, 2016.

[23] L. Bjerkan, A. Røyset, L. Hafskjær, and D. Myhre, "Measurement of laser parameters for simulation of high-speed fiberoptic systems," *J. Lightw. Technol.*, vol. 14, no. 5, pp. 839–850, May 1996.

[24] D. Che, F. Yuan, and W. Shieh, "Towards high-order modulation using complex modulation of semiconductor lasers," *Opt. Express*, vol. 24, no. 6, pp. 6644–6649, 2016.

[25] R. Shafik, S. Rahman, and A. R. Islam, "On the extended relationships among EVM, BER and SNR as performance metrics," in *Proc. IEEE Int. Conf. Elect. Comput. Eng.*, 2006, pp. 408–411.

[26] G. Santella and F. Mazzenga, "A hybrid analytical-simulation procedure for performance evaluation in M-QAM-OFDM schemes in presence of nonlinear distortions," *IEEE Trans. Veh. Technol.*, vol. 47, no. 1, pp. 142–151, Feb. 1998.

[27] B. Hakki, "Evaluation of transmission characteristics of chirped DFB lasers in dispersive optical fiber," *J. Lightw. Technol.*, vol. 10, no. 7, pp. 964–970, Jul. 1992.

[28] G. P. Agrawal, "Optical transmitters," in *Fiber-Optic Fiber Communication Systems*, 4th ed. Hoboken, NJ, USA: Wiley, 2010.

[29] K. K. Loi, J. H. Hodiak, X. B. Mei, C. W. Tu, and W. S. Chang, "Linearization of 1.3-μm MQW electroabsorption modulators using an all-optical frequency-insensitive technique," *IEEE Photon. Technol. Lett.*, vol. 10, no. 7, pp. 964–966, Jul. 1998.

[30] B. Hraimel and X. Zhang, "Performance improvement of radio-over-fiber links using mixed-polarization electro-absorption modulators," *IEEE Trans. Microw. Theory Techn.*, vol. 59, no. 12, pp. 3239–3248, Dec. 2011.

[31] T. Iwai, K. Sato, and K. Suto, "Signal distortion and noise in AM-SCM transmission systems employing the feedforward linearized MQW-EA external modulator," *J. Lightw. Technol.*, vol. 13, no. 8, pp. 1606–1612, Aug. 1995.

[32] Y. Shen, B. Hraimel, X. Zhang, G. E. R. Cowan, K. Wu, and T. Liu, "A novel analog broadband RF predistortion circuit to linearize electro-absorption modulators in multiband OFDM radio-over-fiber systems," *IEEE Trans. Microw. Theory Techn.*, vol. 58, no. 11, pp. 3327–3335, Nov. 2010.

[33] C. H. Cox, III, "Distortion in links," in *Analog Optical Links Theory and Practice*. Cambridge, U.K.: Cambridge Univ. Press, 2004, pp. 201–261.

[34] X. Mao, G. E. Bodeep, R. W. Tkach, A. R. Chraplyvy, T. E. Darcie, and R. M. Derosier, "Brillouin scattering in externally modulated lightwave AM-VSB CATV transmission systems," *IEEE Photon. Technol. Lett.*, vol. 4, no. 3, pp. 287–289, Mar. 1992.

Byung Gon Kim received the B.S. degree in electrical engineering from Hongik University, Seoul, South Korea, in 2014, and the M.S. degree in electrical engineering in 2016 from the Korea Advanced Institute of Science and Technology, Daejeon, South Korea, where he is currently working toward the Ph.D. degree in electrical engineering. His research interest is mobile fronthaul/backhaul networks and analog radio-over-fiber technology.

Sung Hyun Bae received the B.S. degree in electrical engineering from Sogang University, Seoul, South Korea, in 2013, and the M.S. degree in electrical engineering in 2015 from the Korea Advanced Institute of Science and Technology, Daejeon, South Korea, where he is currently working toward the Ph.D. degree in electrical engineering. His research interest is mobile fronthaul/backhaul networks and spatial-division multiplexing technique.

Hoon Kim (SM'11) is currently an Associate Professor with the School of Electrical Engineering, Korea Advanced Institute of Science and Technology (KAIST), Daejeon, South Korea. Prior to joining KAIST in 2014, he was with Bell Labs, Lucent Technologies (2000–2001), Samsung Electronics, South Korea (2001–2007), and National University of Singapore (2007–2014). His research interests include high-capacity fiber-optic communication systems, broadband optical access networks, and mobile fronthaul/backhaul networks. He is currently an Associate Editor for the IEEE PHOTONICS TECHNOLOGY LETTERS and *Optics Express*.

Yun C. Chung (F'06) is currently a professor electrical engineering at Korea Advanced Institute of Science and Technology, Daejeon, South Korea, which he joined in 1994. From 1987 to 1994, he was with the Lightwave Systems Research Department, AT&T Bell Laboratories. From 1985 to 1987, he was with the Los Alamos National Laboratory under the AWU-DOE Graduate Fellowship Program. His current research activities include high-capacity wavelength division multiplexing (WDM) systems and networks, optical performance monitoring techniques, WDM passive optical networks, fiber-optic networks for wireless communications, etc. He has published more than 600 journal and conference papers in these areas and holds more than 90 issued patents. He has served as a General Co-Chair of OFC, OECC, and APOC, as well as the President of the Optical Society of Korea. Prof. Chung is a Fellow of IEEE, OSA, Korean Academy of Science and Technology, and National Academy of Engineering of Korea.